Relationship between Packing Structure and Headgroups of Self-Assembled Monolayers on Au(111): Bridging Experimental Observations through Computer Simulations

Ta-Wei Li, Ito Chao,* and Yu-Tai Tao

Institute of Chemistry, Academia Sinica, Nankang, Taipei 115, Taiwan

Received: November 3, 1997

Computational studies including geometry optimizations and molecular dynamics (MD) simulations are carried out for self-assembled monolayers of *n*-alkanethiols (RSH, R = $C_{16}H_{33}$, $C_{17}H_{35}$) and 4′-alkoxybiphenyl-4-thiols ($ROC_{12}H_8SH$, R = $C_{16}H_{33}$, $C_{17}H_{35}$) on the (111) surface of gold with a full atomic representation force field. In this work, we combine the information derived from scanning tunneling microscopy (STM), surface reflection infrared spectra (IR), and computational studies to uncover the origins of different odd−even effects observed by IR for long chain *n*-alkanethiols and 4′-alkoxybiphenyl-4-thiols and then to establish a relationship between chemical structures of the headgroups and packing structures of thiols on Au(111). Computationally, the odd−even effect is monitored by the relative magnitude of *z*-components (the direction normal to the Au surface) of the methyl group. Although both *n*-alkanethiols and 4′-alkoxybiphenyl-4-thiols occupy the same spacing on Au(111), according to our simulation results, their favored packing structures are different. Because the headgroup of 4′-alkoxybiphenyl-4-thiol ($-SC_{12}H_8O-$) is more rigid than that of *n*-alkanethiol (−S−), 4′-alkoxybiphenyl-4-thiol prefers more structured packing arrangements and thus its odd−even effect is stronger than that of *n*-alkanethiol. In other words, the flexibility of the headgroup greatly influences the variety of possible packing structures. Finally, with this new relationship, we are able to rationalize the strong odd−even effect of a new SAM molecule, *n*-alkyldithioic acid, on Au(111).

1. Introduction

1.1. Packing Arrangements of SAMs and Chemisorption Modes of Sulfur on Au(111). Self-assembled monolayers (SAMs) are currently of considerable interest for fundamental research of interfacial properties as well as technological applications. Typical examples of SAMs are *n*-alkanethiols chemisorbed on Au(111). Owing to simple preparation and highly ordered 2D structures, SAMs of *n*-alkanethiols have served as model systems for the investigation of relationships between molecular structures and surface properties such as wetting,[1−3] In addition, these monolayer films have been modified and used in the design of interfaces for chemical sensing applications,[4] nonlinear optical materials,[5] and surfaces for photopatterning methodology.[6] Nowadays, applications of SAMs have become more sophisticated, so it is important to understand their molecular details in order to engineer the nanoscale surface. The molecular details of *n*-alkanethiols on Au(111) have been extensively studied by various techniques including FTIR,[7] surface-enhanced Raman spectroscopy,[8] diffraction of electrons,[9] X-ray,[10] helium atoms,[11] atomic force microscopy (AFM),[12] and scanning tunneling microscopy (STM).[13−17] However, their actual packing structures and chemisorption mode of sulfur on Au(111) are still unclear.

The earliest model of the packing structures for *n*-alkanethiols chemisorbed on Au(111) was that all of the molecules stood on a lattice of hexagonal ($\sqrt{3} \times \sqrt{3}$)R30 with the same tilt and twist, i.e., one chain per unit cell. Later, at low temperature, Nuzzo et al.[7] observed band splitting in the IR spectra of a docosanethiol ($C = 22$) monolayer on Au, so they suggested that the packing structure of the lowest energy could be a two chains per unit cell structure. Recent studies of both helium diffraction[11] and STM[14] showed a c(4×2) superlattice in addition to the fundamental simple hexagonal ($\sqrt{3} \times \sqrt{3}$)R30 for *n*-alkanethiols on Au(111) (Figure 1). With the aid of the high gap impedance STM, Delamarche et al.[16,17] observed multiple nanoscale domains for *n*-dodecanethiol adsorbed on Au(111), including a simple hexagonal ($\sqrt{3} \times \sqrt{3}$)R30 lattice (as the predominant feature)[16] (Figure 2A) as well as *different* c(4×2) superlattices, where c(4×2) superlattices contain four alkyl chains per unit cell (Figure 2C,D).[16,17]

To find possible packing structures of these different domains for *n*-alkanethiols ($C = 15$) on Au(111), Mar and Klein[18] investigated a model with full atomic representation of methyl and methylene groups. Their simulation results showed a preference for the structure of a two chains per unit cell packing (Figure 2B), whose potential energy was slightly lower than that of a four chains per unit cell packing. The preferred molecular packing structures predicted by Mar and Klein could not explain the contrast variation observed by the high-resolution STM results.[17] The inconsistency between the above simulation results and the STM observation could be caused by neglecting the chemisorption structure of sulfur on Au(111), which is explained as follows. Sellers et al.[19] performed ab initio geometry optimization of HS^- and CH_3S^- on cluster models of Au(111). They found two chemisorption modes, very close in energy, for sulfur atoms on the Au(111) surface. The first mode features an sp^3-hybridization on sulfur, and the equilibrium bond angle of (Au surface)−S−C is ∼104°. The second mode features an sp-hybridization and the equilibrium bond angle is ∼180°.

* Corresponding author. Phone: ++886-2-2789-8530. Fax: ++886-2-2783-1237. E-mail: ichao@chem.sinica.edu.tw.

S1089-5647(98)00049-2 CCC: $15.00
Published on Web 03/31/1998

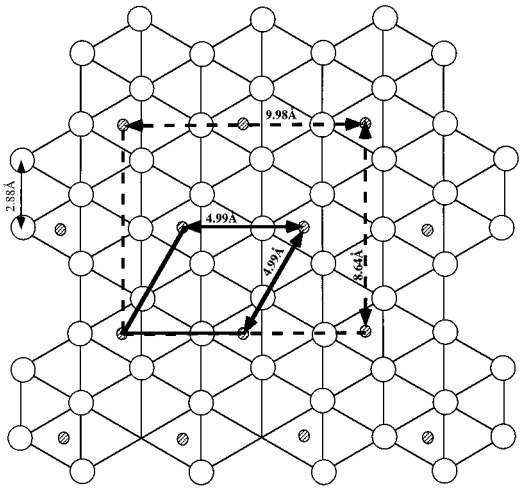

Figure 1. Hexagonal coverage scheme for *n*-alkanethiols and aromatic-derivatized thiols on Au(111). empty circles are gold atoms; shaded circles are sulfur atoms. The space outlined by the thick solid lines is the lattice space of $(\sqrt{3} \times \sqrt{3})$R30° and by the thick dashed lines is the superlattice space of c(4 × 2).

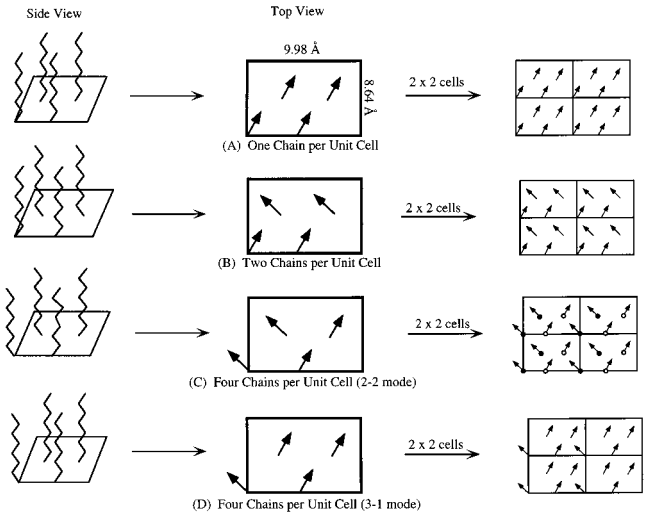

Figure 2. Simplified examples of packing arrangements of *n*-alkanethiols on the superlattice c(4 × 2) include (A) one chain per unit cell, (B) two chains per unit cell, and four chains per unit cell (C) 2−2 mode and (D) 3−1 mode. The arrows represent the projection of the topmost C−C bond. For (C), filled and empty circles were used to differentiate methyl groups with different Z_{CH_3}; see text in Section 4.2.

Using different chemisorption structures (sp- and sp^3-hybridization modes) for sulfur on Au(111), Pertsin and Grunze[20] proceeded with the stochastic global search and energy minimization to explore the most possible packing arrangement for octadecanethiol on Au(111). When there was no predefined chemisorption structure of sulfur on Au(111)—force field I—partly taken from the work of Mar and Klein,[18,21] they found 22 possible packing arrangements within the 1 kcal mol^{-1} energy window of the global minimum. When the chemisorption mode was only sp^3—force field II—four possible packing arrangements were found. When the chemisorption mode was only sp—force field III—six possible ones were found. Finally, when the chemisorption mode was a mixture of sp and sp^3—force field IV—12 possible ones were found. The low-energy packing structures from the force fields I−IV all had tilt angles similar to that deduced from the experimental data, but a different low-energy packing arrangement was promoted if a different chemisorption structure was applied. For example, the lowest energy packing structure from force fields I, II, and IV favored a two chain per unit cell structure, whereas force field III favored a one chain per unit cell structure. Pertsin and Grunze felt that the actual packing structures may have been included in the structures they located. However, without further experimental evidence, it is impossible to screen out unreliable results from grossly defined force fields.

Using the reflection IR spectra, Chang et al. observed a significant difference of the intensity I^z_{sym} of the symmetrical vibration mode of methyl group in the *z*-direction (the direction of the surface normal) from the odd-carbon-number to the even-number *n*-alkanethiols on Au(111),[22] which was termed the odd−even effect. Because I^z_{sym} of the even-number *n*-alkanethiols on Au(111) was greater than that of the odd-number ones, it implied that the chemisorption of sulfur for *n*-alkanethiols on Au(111) should be dominated by the sp^3-hybridization mode. This conclusion is consistent with a previous IR study[7b] and the ab initio study by Sellers et al.[19] In addition, Chang et al. introduced a biphenyl or naphthalene chromophore next to the sulfur atom, which altered the steric requirement of the headgroup. The comparison of the odd−even effect between *n*-alkanethiols and aromatic-derivatized thiols on Au(111) is later found to be quite helpful for solving the relationship between the headgroup and the packing structures.

1.2. Odd−Even Effect of *n*-Alkanethiols and Aromatic-Derivatized Thiols on Au(111). Chang et al.[22] reported the effect of aromatic chromophores on structures of thiols monolayers and compared the monolayer structures of the parent thiols on gold. The reflection IR spectra showed that the aromatic moieties were perpendicular to the Au surface. Although the steric requirement of the headgroup including both a sulfur atom and an aromatic chromophore was quite different from that of a sulfur atom alone, the studies of both high-resolution STM[23] and molecular mechanics calculation[22] indicated that the aromatic-derivatized thiols on Au(111) occupied the same lattice space as *n*-alkanethiols on Au(111). Therefore, the alkyl chains above the aromatic groups were suggested to have similar molecular orientations to *n*-alkanethiols. However, IR spectra of the aromatic-derivatized thiols on Au(111) showed much stronger odd−even effect than *n*-alkanethiols. It implied that the alkyl chains above the aromatic groups have different molecular orientation from those of *n*-alkanethiols on Au(111). How could they have different molecular orientation, while both aromatic-derivatized thiols and *n*-alkanethiols occupy the same lattice on Au(111)? It was postulated that the eclipsing effect of $C_{Ar}-C_{Ar}-O-C$ torsion[24] may result in chain twists of aromatic-derivatized thiols different from those of *n*-alkanethiols. However, exactly how the eclipsing effect influences the packing structure of long alkyl chains, whose cohesive interactions are generally larger than 10 kcal mol^{-1},[25] is unclear.

Moreover, the IR spectra of aromatic-derivatized thiols on Au(111) have clearly shown the diminution of the odd−even effect from short-chain thiols ($C = 4$ and 5) to long-chain thiols ($C = 16$ and 17). Chang et al. proposed that the diminishing of the odd−even effect may be due to progressive rotation of the $C_n-C_{n+1}-C_{n+2}-C_{n+3}$ torsion along alkyl chains. Therefore, the progressive rotation made the methyl ends of the long-chain thiols rotate more than the short-chains thiols and caused the diminishing odd−even effect. If the proposition is correct, why is there no clear diminution of the odd−even effect for *n*-alkanethiols on Au(111)? Walczak et al.[26] also found that the odd−even effect of *n*-alkanethiols on Ag diminished in going from short chains to long chains, where they had a different

TABLE 1: Modified Energy Parameters for θ_{sul} and θ_{ox}[a]

coordinate	$\theta°$	K_θ
$\angle\theta_{sul}$, sp-hybridization[b]	180	2.88
$\angle\theta_{sul}$, sp^3-hybridization[b]	104	46.06
$\angle\theta_{ox}$[c]	115	350.00

[a] $\theta°$ is the equilibrium angle, and the unit is deg. K_θ is the force constant, and the unit is kcal mol^{-1} rad^{-2}. [b] See ref 19. [c] The ab initio study (ref 24) of anisole showed that the rotational barrier of ϕ_{ox} is 2.1 kcal mol^{-1}; θ_{ox} is 119.8° when ϕ_{ox} is 0°, and θ_{ox} is 115.5° when ϕ_{ox} is 90°. Our model shows that the rotational barrier of ϕ_{ox} is 2.18 kcal mol^{-1}; θ_{ox} is 119.6° when ϕ_{ox} is 0°, and θ_{ox} is 116.8° when ϕ_{ox} is 90°.

proposition; i.e., the SAM films may adopt different structures from short chains to long chains.

On the basis of the previous observations from STM and IR studies, we use computational techniques to investigate the molecular orientations of the multiple packing structures (domains) and the enhanced odd−even effect in going from *n*-alkanethiols to aromatic-derivatized thiols. In this article, calculations including molecular mechanics and molecular dynamics (MD) simulations are reported for *n*-alkanethiols (C = 16, 17) and 4′-alkoxybiphenyl-4-thiols (C = 16, 17) on the Au(111) surface with a full atomic representation force field.[27] First, we search the possible packing structures of *n*-alkanethiols and 4′-alkoxybiphenyl-4-thiols on Au(111) for different molecular domains, i.e., one chain, two chains, and four chains per unit cell at 0 K. Then, we statistically analyze their thermal motions at 298 K. In the end, with the simulation results, we explore the relation between the packing arrangements and chemical structures of headgroups of SAMs, which could provide useful insight for the rational molecular design of surface properties.

2. Molecular Model

In the computer simulations of SAMs of *n*-alkanethiols and aromatic-derivatized thiols, it is desirable to treat hydrogen atoms explicitly in order to obtain the correct packing structure. An all-atom model, the DREIDING2.21 force field,[28] is applied with partial charges obtained from the Mulliken charges of AM1[29] calculations (see Supporting Information). In addition, the DREIDING2.21 force field is modified to fit the quantum mechanics calculation results of the torsional barrier around $O-C_{Ar}$ (ϕ_{ox})[24] and chemisorption structures of sulfur on Au(111).[19] The torsional energy of ϕ_{ox} (barrier around $O-C_{Ar}$) is written as

$$E_\phi = {}^1/_2 k_\phi[1 - \cos(2\phi)] \quad (1)$$

where k_ϕ is 18 kcal mol^{-1}. The potential energies of bending angles centered on sulfur and oxygen atoms, θ_{sul} and θ_{ox}, are described as a simple θ harmonic function written as the following equation

$$E_\theta = {}^1/_2 K_\theta(\theta - \theta°)^2 \quad (2)$$

where K_θ is the force constant and $\theta°$ is the equilibrium bond angle. The potential parameters of θ_{sul} and θ_{ox} are shown in Table 1, including both chemisorption modes of S on Au(111)—sp^3- and sp-hybridizations. Results from ab initio calculations showed that the energy difference between these two modes is small,[19] and in our model it is assumed to be zero. It should be noted that sulfur atom on the Au(111) surface is believed to bind on the hollow site but not on the top of a gold atom (Figure 1).[19] In our model of SAMs, a virtual atom H is assigned to be the center of the hollow site. Both sulfur and H are fixed in the lattice spacing of ($\sqrt{3} \times \sqrt{3}$)R30°, and the bond, $H-S$, is normal to the gold surface. This simplified fixed model was used in view of the same packing spacing of long chain *n*-alkanethiols and aromatic-derivatized thiols revealed by STM investigations.[14,16,17,23]

3. Computational Details

3.1. Geometry Optimization Calculations. All of the calculations, including both geometry optimizations and molecular dynamics simulations, are carried out with the program Cerius[2] v2.0.[30] For geometry optimization, the SAM systems are studied with periodical models in which each box contains four SAM molecules. The geometric parameters of a sampling box are a = 9.98 Å, b = 8.64 Å, c = 60 Å and $\alpha = \beta = \gamma$ =90°, which is the superlattice spacing of c(4 × 2). The length of the *c*-axis was set as 60 Å to mimic two-dimensional surface monolayers. The spline cutoff method is used for the calculation of nonbonded interactions. The spline is on at 8.0 Å and off at 8.5 Å. The SAM molecules in the superlattice spacing are modeled with different packing arrangements including one chain per unit cell, two chains per unit cell, and four chains per unit cell (examples shown in Figure 2). The minimization algorithm is the conjugated gradient method with the termination criteria of the residual root-mean-square (rms) force 0.005 kcal mol^{-1} $Å^{-1}$.

According to the odd−even effect observed by Chang et al.,[22] we first search the low-energy packing arrangements with the sp^3 chemisorption mode for *n*-alkanethiols on Au(111). Reflection infrared (IR) spectroscopy has indicated high-density crystalline-like packing as well as the all-trans conformation of the alkyl chains. According to a fit of calculated IR spectral intensities to the experimentally observed IR spectra, the tilt, θ, of the alkyl chain from the surface normal is 33° and the twist, ϕ, of the alkyl chain plane is 55°.[7] (See List of Symbols for detailed descriptions of θ and ϕ.) In addition, Mar and Klein[18] showed that $\theta \approx 30°$, $\phi \approx 50°$, alkyl chains lean toward the next nearest neighbor, and Pertsin and Grunze[20] also pointed out that θ = 30°−40° and $\phi \approx \pm 50°$ or $\pm 130°$ in general. Therefore, the initial tilts, θ, are set as 30° and their alkyl chains are toward the next nearest neighbor for the initial packing structures of the geometry optimization calculations. Meanwhile, with different combination of ϕ (either $\pm 50°$ or $\pm 130°$), we obtain the different initial packing structures for *n*-alkanethiols on Au(111).

In the packing study[22,31] of biphenyl with a para hydrogen constrained on a two-dimensional plane, it was concluded that biphenyl stood nearly normal to the surface, occupying a ($\sqrt{3} \times \sqrt{3}$)R30° Au(111) lattice instead of p(2 × 2), and preferred a herringbone arrangement instead of a face-stacked arrangement. Subsequent STM study of oligo(phenylethynyl)benzenethiols also gave results consistent with a herringbone arrangement;[23] therefore, only herringbone packing arrangement of biphenyl-4-thiols on the superlattice c(4 × 2) is considered (Figure 3). For alkoxybiphenyl-4-thiols, we use the optimized biphenyl-4-thiols as the headgroups and connect alkyl chains with oxygen atoms. Similar to the case of *n*-alkanethiols, we set all θ to be 30° and their alkyl chains toward the next nearest neighbor. Then, we change ϕ to $\pm 50°$ or $\pm 130°$ to obtain the different initial packing structures of 4′-alkoxybiphenyl-4-thiols on Au(111).

3.2. Details of Molecular Dynamics (MD) Simulations. In the MD simulations, the SAM systems are studied in the canonical (NVT) ensemble at constant temperature 298 K with the Nosé method.[32] Every sampling system contains the

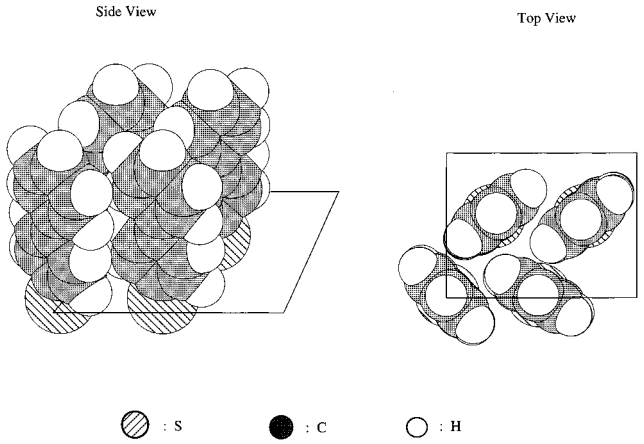

Figure 3. Herringbone packing arrangement of biphenyl on the superlattice c(4 × 2).

periodical boundary condition with a box containing 16 SAM molecules. The typical total sampling time is 130 ps in a time step of 0.001 ps, and the statistical analyses are done over 70 ps after the equilibration phase of the first 60 ps. As in the geometry calculations, the spline cutoff method is used for the calculation of nonbonded interactions. The spline is on at 8.0 Å and off at 8.5 Å. The initial configurations of MD simulations are the final results of the geometry optimizations.

It is noted that the sampling box contains only 16 molecules. One may wonder whether the sampling system is too small to capture correct structural features of thiols on Au(111). Siepmann and McDonald[33] have extensively studied the system-size dependence in simulations of *n*-hexadecanethiol on Au(111). They reported that $\langle Z_{tail} \rangle$ the mean distance between the terminal methyl group and the Au surface in the *z*-direction (the direction of the surface normal), was apparently a weak function of the system size. Herein, our MD simulations focus on the study of $\langle Z_{CH_3} \rangle$, the *z*-projection of the methyl groups. Since $\langle Z_{CH_3} \rangle$ and $\langle Z_{tail} \rangle$ have the similar dimensionality, $\langle Z_{CH_3} \rangle$ is assumed to be a weak function of the system size.

4. Results and Discussion

4.1. Packing Structure at 0 K: Geometry Optimization Results. As deduced from the odd−even effect observed by previous IR experimental results, the chemisorption modes in simulation studies are established with sp^3-hybridization for *n*-alkanethiols and sp hybridization for 4′-alkoxybiphenyl-4-thiols on Au(111). After extensive search, there are four stable packing arrangement (which do not change to some orderless structures) found for *n*-alkanethiols with sp^3 chemisorption on Au(111), i.e., packing structures A, B, C, and D in Table 2, which is similar to the results of Pertsin and Grunze.[20] For *n*-alkanethiols (C =16 and 17), packing structure A (Figure 4A) is one chain per unit cell with all of the twist angles, ϕ, around 36° and packing structure B (Figure 4B) is two chains per unit cell with half of ϕ around 50° and another half around −50°. Packing structures C and D are two different types of four chains per unit cell, which are the 2−2 mode and the 3−1 mode, respectively. For the 2−2 mode, half of the ϕ are around 45° and the other half are around 130°; for the 3−1 mode, $^3/_4$ of the ϕ are around 40° and $^1/_4$ are around 130°. Among these four packing structures of *n*-alkanethiols on Au(111), one chain per unit cell has the lowest energy for C = 16 and 17.[34] For packing structure C in Table 2, there are two θ_{sul} (bending angles of sulfur) larger than 120° whose ϕ are both ca. 130°. It is suspected that these two twists produce large intermolecular repulsion and cause large deviation of θ_{sul} from the equilibrium angle of the sp^3-hybridization mode, 104°. Because the force constant of θ_{sul} of the sp^3-hybridization mode is significantly larger than that of the sp mode (Table 1),[19] the energy penalty produced by the large deviation of θ_{sul} (which may cause the total potential energy of packing structure C being higher than that of packing structure A) can be reduced by replacing the chemisorption hybridization from the sp^3 mode to the sp mode. After replacement, the potential energy of the 2−2 mode is indeed lowered (see packing structure E in Table 2 and Figure 4C). It is noted that θ_{sul} of the sp mode in packing structure E is around 145°, which deviates significantly from the equilibrium angle (180°). Because the force constant of the sp-hybridization mode is much smaller than that of the sp^3-hybridization mode[19] such a large bending does not produce a large energy penalty (please see Figure 5, and more discussion will be given in the next paragraph). The same replacement of the chemisorption modes for the 3−1 mode of four chains per unit cell packing also lowered the potential energy of the new 3−1 mode (structure F in Table 2 and Figure 4D). In addition, it is conceivable that if alkyl chains can pack in the 3−1 mode, a nearly equivalent packing arrangement for the alkyl chains could be a 1−3 mode. Therefore, in an attempt to locate a 1−3 mode, we set three sulfur atoms to be in the sp-hybridization mode

TABLE 2: Geometry Optimization Results of *n*-Alkanethiols on Au(111)[a]

packing structures: chemisorption modes		C = 16	C =17
A. 1 chain per unit cell: all sp^3	ΔE	0.00	0.00
	θ	29.1	29.1
	ϕ (θ_{sul})	36.1 (115.7)	36.1 (115.7)
B. 2 chains per unit cell: all sp^3	ΔE	4.10	4.50
	θ	29.9	29.8
	ϕ (θ_{sul})	50.3 (114.9)	48.4 (114.9)
		−50.3 (114.9)	−48.4 (114.9)
C. 4 chains per unit cell (2−2 mode): all sp^3	ΔE	4.50	4.79
	θ	30.6	30.4
	ϕ (θ_{sul})	44.4 (117.1)	44.9 (114.4)
		44.4 (114.3)	45.5 (117.0)
		130.7 (125.7)	130.6 (125.8)
		133.2 (121.2)	132.6 (121.0)
D. 4 chains per unit cell (3−1 mode): all sp^3	ΔE	3.38	3.59
	θ	30.5	30.3
	ϕ (θ_{sul})	37.9 (115.2)	37.9 (115.2)
		40.4 (114.2)	41.1 (116.7)
		43.2 (116.7)	43.3 (114.3)
		132.5 (123.7)	132.1 (123.4)
E. 4 chains per unit cell (2−2 mode): half sp^3 and half sp	ΔE	1.98	2.27
	θ	30.3	30.2
	ϕ (θ_{sul})	47.5 (118.1)	49.2 (118.0)
		47.8 (120.3)	49.2 (119.9)
		131.4[b] (144.5)	131.4[b] (144.6)
		133.4[b] (144.5)	133.1[b] (145.4)
F. 4 chains per unit cell (3−1 mode): $^3/_4$ sp^3 and $^1/_4$ sp	ΔE	2.15	2.35
	θ	30.7	30.7
	ϕ (θ_{sul})	39.0 (116.7)	39.3 (116.7)
		40.7 (118.3)	41.5 (118.3)
		44.5 (116.3)	44.5 (116.3)
		132.7[b] (143.3)	132.2[b] (143.3)
G. 4 chains per unit cell (1−3 mode): $^1/_4$ sp^3 and $^3/_4$ sp	ΔE	2.44	2.90
	θ	30.3	30.3
	ϕ (θ_{sul})	−48.7 (121.6)	−48.8 (121.5)
		−139.7[b] (153.3)	−138.8[b] (153.5)
		−137.7[b] (150.0)	−135.6[b] (150.1)
		−137.9[b] (151.3)	−135.9[b] (151.4)

[a] $\Delta E = E - E$(one chain per unit cell), and E is the potential energy per chain. Units: ΔE, kcal mol^{-1}; θ and ϕ, deg. [b] The chemisorption mode of S is sp-hybridization.

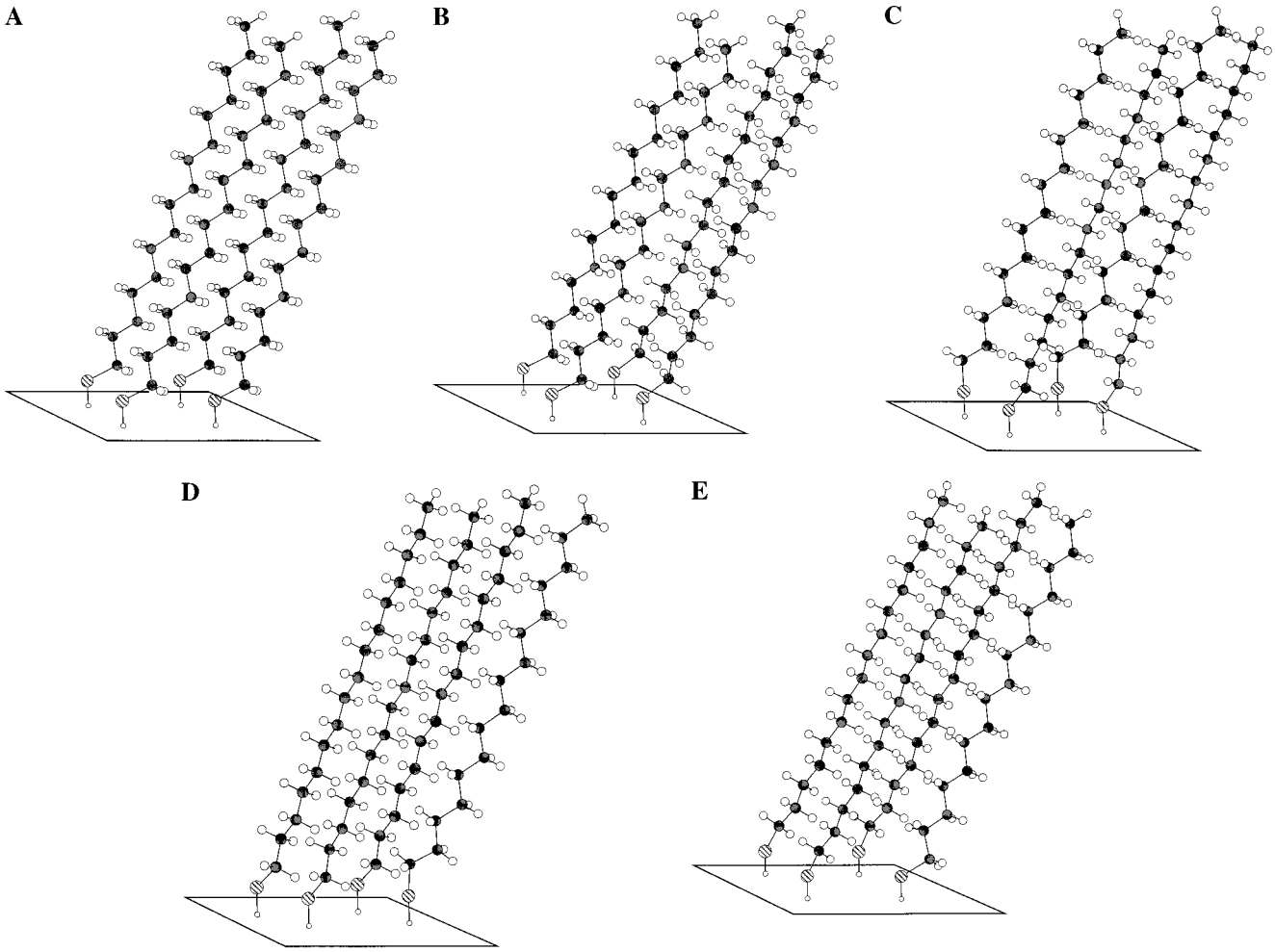

Figure 4. Molecular structures of various packing structures for *n*-alkanethiols on Au(111): (A) one chain per unit cell (all sp^3 chemisorption), (B) two chains per unit cell (all sp^3 chemisorption), (C) four chains per unit cell (2−2 mode; half sp and half sp^3 chemisorption), (D) four chains per unit cell (3−1 mode; $^1/_4$ sp and $^3/_4$ sp^3 chemisorption), and (E) four chains per unit cell (1−3 mode; $^3/_4$ sp and $^1/_4$ sp^3 chemisorption).

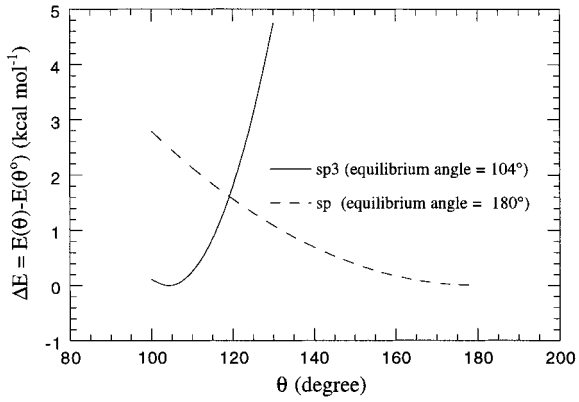

Figure 5. Bending energy profiles of θ_{sul} with respect to sp^3 and sp chemisorption modes of S on Au(111).

and find another local minima for four chains per unit cell packing, the 1−3 mode. (structure G, Figure 4E).[35]

To understand how the change of the hybridization mode of θ_{sul} from sp^3 to sp influences the packing structure of four chains per unit cell (2−2 mode), we examine the energy difference between packing structures C and E in Table 2 for *n*-alkanethiols ($C = 17$). The total energy difference, ΔE(total), between these two structures is 2.52 kcal mol^{-1} (Table 3) and can be decomposed into three parts including the nonbonded interaction, ΔE(nonbonded), the bending energy of θ_{sul}, ΔE(chemisorption), and the intramolecular steric energy, ΔE(intramolecular). It can be seen in Table 3 that all three energy components contribute to the energy lowering from structure C to structure E. Therefore, it implies that the change of chemisorption mode of θ_{sul} from the sp^3 mode to the sp mode not only changes the rigidity of θ_{sul} but also allows better chain−chain interaction and in the meantime relieves the intramolecular strain produced by the 2−2 four chains per unit cell packing mode.

The packing structures from the minimization results of 4′-alkoxybiphenyl-4-thiols on Au(111) are summarized in Table 4. All structures have the basic herringbone packing pattern in the biphenyl part, so only structure parameters of the alkoxy part are shown. The bending angles around oxygen, θ_{ox}, are ca. 120°, which is close to the equilibrium angle of anisole described in Table 1 (see footnote *c* of Table 1). It is found that one chain per unit cell packing is the most favorable one for both $C = 16$ and 17, as what has been found for *n*-alkanethiols on Au(111). Interestingly, the $C_{Ar}-C_{Ar}-O-C$ torsional angles, ϕ_{ox}, of packing structure B (two chains per unit cell packing for the alkyl part) in Table 4 are either around 18° or −18°, which are both close to the global minimum at $\phi_{ox} = 0°$. And, ϕ_{ox} of packing structure A (one chain per unit cell for the *alkyl* part) in Table 4 are either 18° or 80°, where 18° is close to the minimum at $\phi_{ox} = 0°$ and 80° to the local maximum at 90°. In four chains per unit cell structures (C and D), one half of the ϕ_{ox} are close to the minimum and the other

TABLE 3: Analysis of Energy Difference between Packing Structures C and E in Table 2 for *n*-Alkanethiols ($C = 17$)[a]

	ΔE(total)	ΔE(nonbonded)	ΔE(chemisorption)	ΔE(intramolecular)
$\Delta E = E$(structure C) $- E$(structure E)	2.52	0.68	≈0.64	≈1.20

[a] The nonbonded part includes the intermolecular interaction of van der Waals and electrostatic energies. The chemisorption part is calculated from the bending energy of θ_{sul} as in Figure 5, and the remaining energy difference is summarized as the intramolecular part. Units: kcal mol^{-1}.

TABLE 4: Geometry Optimization Results of 4′-Alkoxybiphenyl-4-thiols on Au(111)[a]

packing structures: chemisorption modes		$C = 16$	$C = 17$
A. 1 chain per unit cell: all sp	ΔE	0.00	0.00
	θ	28.1	28.2
	ϕ (ϕ_{ox}) θ_{ox}	37.4 (18.0) 118.9	37.5 (18.5) 117.1
		37.4 (−80.8) 117.2	37.5 (−79.4) 118.8
B. 2 chains per unit cell: all sp	ΔE	1.37	1.93
	θ	27.5	27.6
	ϕ (ϕ_{ox}) θ_{ox}	44.4 (18.5) 119.1	44.1 (18.4) 119.1
		−46.8 (−18.8) 119.2	−46.6 (−18.6) 119.2
C. 4 chains per unit cell (2−2 mode): all sp	ΔE	1.29	1.74
	θ	29.5	29.4
	ϕ (ϕ_{ox}) θ_{ox}	44.6 (12.3) 118.9	46.0 (12.3) 118.8
		44.7 (−71.7) 116.8	46.4 (−71.6) 116.9
		127.1 (58.6) 119.8	127.0 (58.5) 119.8
		130.3 (−15.9) 121.6	130.0 (−15.9) 121.6
D. 4 chains per unit cell (3−1 mode): all sp	ΔE	1.37	1.76
	θ	28.9	28.8
	ϕ (ϕ_{ox}) θ_{ox}	37.5 (15.6) 118.8	37.6 (14.7) 118.9
		39.8 (−70.8) 117.5	40.2 (−71.2) 117.4
		42.3 (−76.1) 117.0	43.1 (−76.2) 117.0
		129.8 (−11.3) 121.9	129.5 (−10.2) 121.8

[a] The assigned packing arrangement of 4′-alkoxybiphenyl-4-thiols is concerned only with the alkyl chains. $\Delta E = E - E$(one chain per unit cell), and E is the potential energy. θ and ϕ are the tilt and the twist of alkyl chains. Units: ΔE, kcal mol^{-1}; θ and ϕ, deg.

half to the maximum. Hence, it is suspected that the eclipsing effect of the $C_{Ar}-C_{Ar}-O-C$ torsion may affect the energy of two chains per unit cell relative to one chain per unit cell and to four chains per unit cell structures. For the 4′-alkoxybiphenyl-4-thiols, the cohesive energy of alkyl chains in one chain per unit cell is estimated to be around 4 kcal mol^{-1} larger than that in two chains per unit cell.[36] This energy difference is larger than the torsional energy barrier of ϕ_{ox} (2.1 kcal mol^{-1}), so the eclipsing effect does not change the preferred packing structure of the long-chain 4′-alkoxybiphenyl-4-thiols. And the potential energy of one chain per unit cell is lower than the other packing arrangement, which is similar to the case of *n*-alkanethiols.

4.2. Packing Structures at 298 K: Molecular Dynamics (MD) Simulations. On the basis of the STM observation of multiple nanoscale domains for the dodecanethiol SAM on Au(111),[16,17] our MD simulations focus on molecular behavior of the individual domain at 298 K. All of the properties, including the potential energies, the tilts, and the twists of alkyl chains, reach their equilibrium values within the 60-ps equilibration phase.[37] Tables 5 and 6 show the statistically average properties of every packing structure obtained from the MD results of *n*-alkanethiols and 4′-alkoxybiphenyl-4-thiols on Au(111). For both *n*-alkanethiols and 4′-alkoxybiphenyl-4-thiols on Au(111), the potential energy of one chain per unit cell is the lowest one among the different packing structures. In addition, the clear distinction of the averaged potential energies and geometric parameters among different packing arrangements shows that most of the SAMs are still in their local minima at 298 K. An interesting exception in Table 5 is that the energy of packing structure C is almost the same as packing structure A for both $C = 16$ and 17. Figure 6A,C shows that both of them have similar population profiles of ϕ at 298 K, in which only one peak are observed. Therefore, the 2−2 mode of four chains per unit cell packing with pure sp^3 chemisorption structure (structure C) is unstable and transformed into one chain per unit cell at the ambient temperature condition. Nevertheless, when half of sulfur atoms have sp^3-hybridization and the other half have sp-hybridization, the 2−2 mode is stable at 298 K. (See Figure 6E and structure E in Table 5.) The reasons why the 2−2 mode with pure sp^3 chemisorption is unstable could be traced back to unfavorable interchain and intrachain interactions, as already discussed in the previous section (Table 3). In other words, a mixture of chemisorption of sp^3- and sp-hybridization provides a flexible headgroup to stabilize the 2−2 mode of four chains per unit cell packing for *n*-alkanethiols on Au(111) at both 0 and 298 K, which does not occur when the chemisorption structures are all of sp^3-hybridization. The same situation also occurs for the 1−3 mode of four chains per unit cell packing.[35] Therefore, the flexibility of a sulfur headgroup plays an important role to stabilize various packing structures for superlattices of *n*-alkanethiols on Au(111).

One of the important reasons to run MD simulations is to study the odd−even effect of the SAMs on Au(111) at 298 K. In our previous work,[22] using reflection IR spectroscopy to investigate SAMs on Au(111), one can easily observe that I^z_{sym} of $C =$ odd number is distinctly different from $C =$ even number (the odd−even effect). Since I^z_{sym} is directly related to $\langle Z_{CH_3}\rangle$, the averaged *z*-projection of the methyl group (see List of Symbols), the odd−even effect can be characterized as the change of $\langle Z_{CH_3}\rangle$ from the odd-carbon-number SAMs to the even-carbon-number, which can be readily calculated from the MD simulation results. As shown in Tables 7 and 8, the change of the *z*-projection of the methyl group from $C = 16$ to $C = 17$, $\delta\langle Z_{CH_3}\rangle$ ($=\langle Z_{CH_3}\rangle_{C17} - \langle Z_{CH_3}\rangle_{C16}$), is strongly influenced by the packing arrangement of the alkyl part; one chain per unit cell packing shows the strongest odd−even effect ($\delta\langle Z_{CH_3}\rangle = -0.43$ Å), followed by two chains per unit cell ($\delta\langle Z_{CH_3}\rangle = -0.34$ to -0.32 Å) and 3−1 mode of the four chains per unit cell packing ($\delta\langle Z_{CH_3}\rangle = -0.23$ to -0.22 Å). The 2−2 mode of

TABLE 5: MD Simulation Results of *n*-Alkanethiols on Au(111) at 298 K[a]

initial packing structures: chemisorption modes		$C = 16$	$C = 17$
A. 1 chain per unit	$\Delta\langle E\rangle$	0.0 ± 1.2	0.0 ± 1.3
cell: all sp^3	$\langle\theta\rangle$	29.3 ± 0.5	29.3 ± 0.8
	$\langle\phi\rangle$	37 ± 10	38 ± 10
	$\langle Z_{CH_3}\rangle$	1.07 ± 0.10	0.64 ± 0.11
B. 2 chains per unit	$\Delta\langle E\rangle$	3.2 ± 1.3	3.5 ± 1.3
cell: all sp^3	$\langle\theta\rangle$	29.6 ± 0.8	29.6 ± 0.6
	$\langle\phi\rangle$	$\pm 53 \pm 12$	$\pm 51 \pm 11$
	$\langle Z_{CH_3}\rangle$	1.05 ± 0.11	0.71 ± 0.13
C. 4 chains per unit	$\Delta\langle E\rangle$	0.3 ± 1.3	0.2 ± 1.0
cell (2−2 mode):	$\langle\theta\rangle$	30 ± 1	30 ± 1
all sp^3	$\langle\phi\rangle$	39 ± 11	39 ± 10
	$\langle Z_{CH_3}\rangle$	1.07 ± 0.18	0.64 ± 0.11
D. 4 chains per unit	$\Delta\langle E\rangle$	3.1 ± 1.3	3.2 ± 1.3
cell (3−1 mode):	$\langle\theta\rangle$	30 ± 1	30 ± 1
all sp^3	$\langle\phi\rangle$	40 ± 11	40 ± 10
		133 ± 10	133 ± 9
	$\langle Z_{CH_3}\rangle$	0.98 ± 0.12	0.75 ± 0.21
E. 4 chains per unit	$\Delta\langle E\rangle$	2.0 ± 1.3	2.1 ± 1.3
cell (2−2 mode):	$\langle\theta\rangle$	29 ± 2	29 ± 1
half sp^3 and half sp	$\langle\phi\rangle$	45 ± 11	45 ± 10
		135 ± 10	135 ± 9
	$\langle Z_{CH_3}\rangle$	0.86 ± 0.22	0.86 ± 0.22
F. 4 chains per unit	$\Delta\langle E\rangle$	1.9 ± 1.3	2.0 ± 1.4
cell (3−1 mode):	$\langle\theta\rangle$	29 ± 2	29 ± 2
$^3/_4$ sp^3 and $^1/_4$ sp	$\langle\phi\rangle$	39 ± 12	35 ± 12
		133 ± 9	125 ± 11
	$\langle Z_{CH_3}\rangle$	0.98 ± 0.18	0.75 ± 0.21
G. 4 chains per unit	$\Delta\langle E\rangle$	2.0 ± 1.3	2.4 ± 1.3
cell (1−3 mode):	$\langle\theta\rangle$	29 ± 1	29 ± 1
$^1/_4$ sp^3 and $^3/_4$ sp	$\langle\phi\rangle$	-49 ± 10	-50 ± 10
		-139 ± 11	-139 ± 10
	$\langle Z_{CH_3}\rangle$	0.75 ± 0.21	0.97 ± 0.19

[a] The initial packing structures are obtained from the geometry optimization results (Table 2). $\Delta\langle E\rangle = \langle E\rangle - \langle E(\text{one chain per unit cell})\rangle$, and E is the potential energy. Units: $\Delta\langle E\rangle$, kcal mol^{-1}; $\langle\theta\rangle$ and $\langle\phi\rangle$, deg; $\langle Z_{CH_3}\rangle$, Å.

TABLE 6: MD Simulation Results of 4′-Alkoxybiphenyl-4-thiols on Au(111) at 298 K[a]

initial packing structures: chemisorption modes		$C = 16$	$C = 17$
A. 1 chain per unit	$\Delta\langle E\rangle$	0.0 ± 1.6	0.0 ± 1.3
cell: all sp	$\langle\theta\rangle$	27 ± 2	27 ± 2
	$\langle\phi\rangle$	33 ± 11	32 ± 11
	$\langle Z_{CH_3}\rangle$	1.05 ± 0.12	0.63 ± 0.17
B. 2 chains per unit	$\Delta\langle E\rangle$	1.8 ± 1.6	1.8 ± 1.3
cell: all sp	$\langle\theta\rangle$	26 ± 2	26 ± 2
	$\langle\phi\rangle$	$\pm 47 \pm 14$	$\pm 46 \pm 13$
	$\langle Z_{CH_3}\rangle$	1.04 ± 0.10	0.72 ± 0.18
C. 4 chains per unit	$\Delta\langle E\rangle$	2.45 ± 1.6	2.68 ± 1.6
cell (2−2 mode):	$\langle\theta\rangle$	27 ± 2	27 ± 2
all sp	$\langle\phi\rangle$	36 ± 12	35 ± 13
		123 ± 12	123 ± 12
	$\langle Z_{CH_3}\rangle$	0.86 ± 0.21	0.86 ± 0.21
D. 4 chains per unit	$\Delta\langle E\rangle$	2.1 ± 1.6	2.1 ± 1.3
cell (3−1 mode):	$\langle\theta\rangle$	28 ± 2	28 ± 2
all sp	$\langle\phi\rangle$	34 ± 13	35 ± 12
		124 ± 11	125 ± 11
	$\langle Z_{CH_3}\rangle$	0.98 ± 0.17	0.76 ± 0.16

[a] The assigned packing arrangement of 4′-alkoxybiphenyl-4-thiols is concerned only with the alkyl chains. The initial packing structures are obtained from the geometry optimization results (Table 4). $\Delta\langle E\rangle = \langle E\rangle - \langle E(\text{one chain per unit cell})\rangle$, and E is the potential energy. Units: $\Delta\langle E\rangle$, kcal mol^{-1}; $\langle\theta\rangle$ and $\langle\phi\rangle$, deg; $\langle Z_{CH_3}\rangle$, Å.

four chains per unit cell shows zero odd−even effect, and the 1−3 mode shows opposite odd−even effect ($\delta\langle Z_{CH_3}\rangle = 0.22$ Å). The close resemblance of the odd−even effect between *n*-alkanethiols and 4′-alkoxybiphenyl-4-thiols of a given packing structure is worth some comments. It implies that the packing of the alkyl part dictates the odd−even effect of a given domain, whereas the molecular fragment below the alkyl part (i.e., the headgroup) seems to play a lesser role in this respect. Nevertheless, the headgroups may play roles in determining the relative population between *different* domains.

How does the packing arrangement influence $\delta\langle Z_{CH_3}\rangle$, the odd−even effect? First, it is noted that the alkyl chains of *n*-alkanethiols and 4′-alkoxybiphenyl-4-thiols on Au(111) are basically in the trans-zigzag conformation, which has been indicated by the reflection IR spectra.[22] Second, the control of the magnitude of $\langle Z_{CH_3}\rangle$ is made up of two parts: $\langle\theta\rangle$ and $\langle\phi\rangle$. Since Tables 5 and 6 show that $\langle\theta\rangle$ are always around 30°, the change of the magnitude of $\langle Z_{CH_3}\rangle$ is mainly dependent on the twists of their alkyl chains. Here, we take C = even and odd of *n*-alkanethiols as an example (Figure 7) to discuss the relationship between $\langle\phi\rangle$ and the odd−even effect of *n*-alkanethiols on Au(111). First, we define the zero twist of a alkyl chain as in Figure 7A, where the chemisorption of sulfur is in sp^3 hybridization and the alkyl chain plane is without any twist. When the carbon number is odd, the vector of the methyl group tilts away from the *z*-axis (the surface normal); when the carbon number is even, the vector of the methyl group is almost parallel to the *z*-axis. Therefore, $\langle Z_{CH_3}\rangle$ of the odd-carbon-number alkyl chain is smaller than that of the even-carbon-number one and so is I^z_{sym}. As the twist, ϕ, of the alkyl chain increases, the vector of the methyl group of the odd-carbon-number chain starts to tilt close to the surface normal and the vector of the methyl group of the even-carbon-number chain starts to tilt away from the surface normal. When the twist of alkyl chain reaches 90° as shown in Figure 7B, $\langle Z_{CH_3}\rangle$ of the odd-carbon-number chain is equal to that of the even-carbon-number one. At this time, one could observe identical I^z_{sym} for both the odd and even-carbon-number chain, so there is no odd−even effect. As the twist of alkyl chain continues to increase, the vector of the methyl group of the odd-carbon-number chain continues to tilt close to the surface normal and the vector of the methyl group of the even-carbon-number chain continues to tilt away from the surface normal. When the twist of alkyl chain reaches 180° as shown in Figure 7C, the vector of the methyl group for the odd-carbon-number chain is almost parallel to the *z*-axis and the vector of the methyl group for the even-carbon-number chain tilts away from the *z*-axis to the maximum point, which is just opposite to the situation of the zero twist. Consequently, the odd−even effect of the 180° twist is opposite to the zero twist and so is $\delta\langle Z_{CH_3}\rangle$. A short summary of the odd−even effect with respect to the twist of a alkyl chain is given below. It is noted that this summary is based on two assumptions: the alkyl chain is in the trans-zigzag conformation, and its tilt angle is fixed.

(1) With the same magnitude but different sign of ϕ, Z_{CH_3}'s of alkyl chains are the same. For example, Z_{CH_3} of the twist of 50° is equal to the twist of −50°, so their odd−even effects are the same.

(2) The odd−even effect of ϕ between 0° and 90° is opposite to the odd−even effect of ϕ between 90° and 180°; e.g., the odd−even effect of the twist of 45° is opposite to the twist of 135°. Similarly, the odd−even effect of ϕ between 0° and −90° is opposite to the odd−even effect of ϕ between −90° and −180°.

(3) No matter what the twist is (either greater than 90° or smaller than 90°), the closer it approaches to 90°, the weaker the odd−even effect will be. When ϕ is either 0° or 180°, the

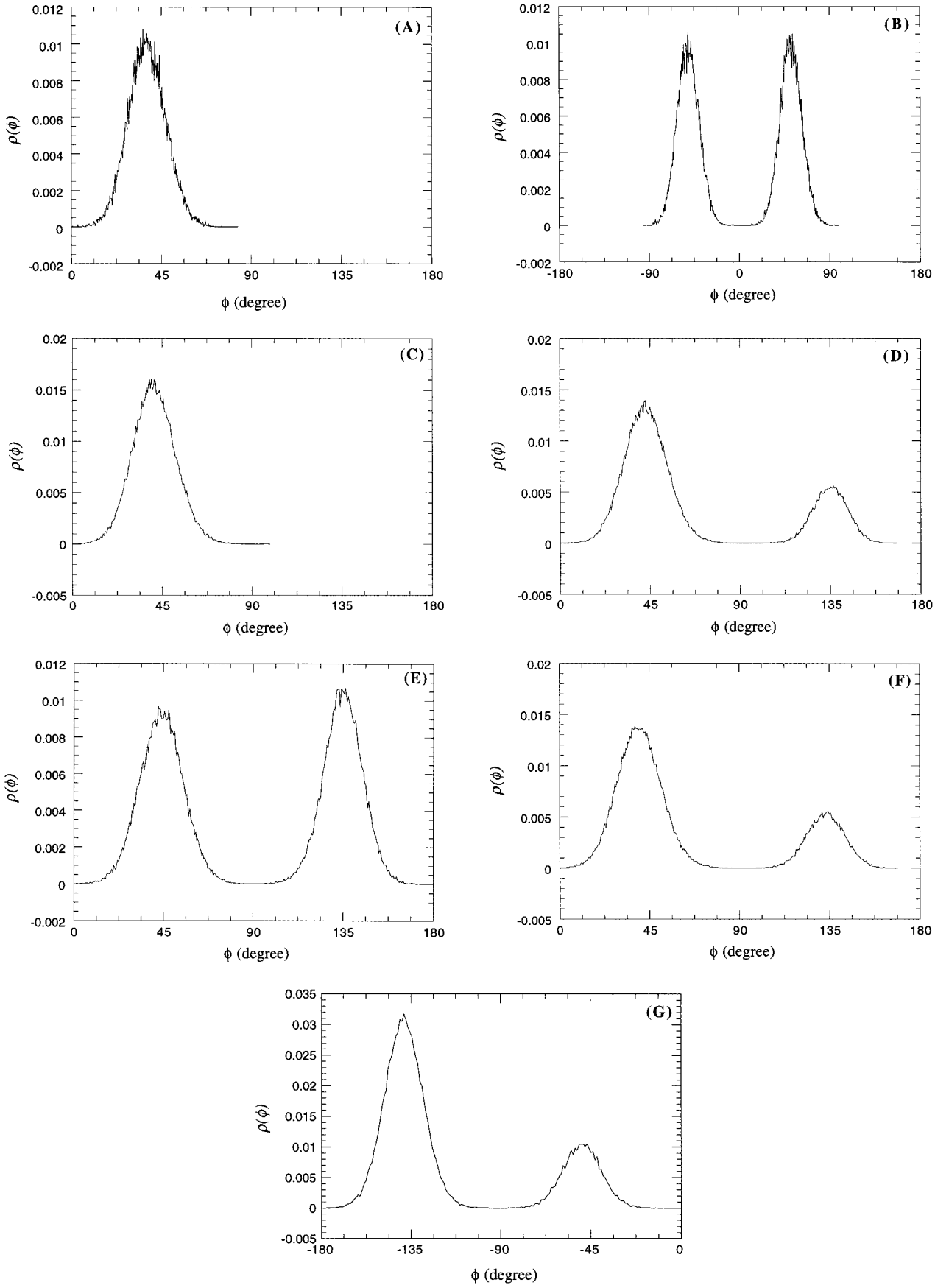

Figure 6. Population profiles of twist angles of different packing arrangements for long-chain ($C = 17$) SAMs of alkanethiols: (A) one chain per unit cell (all sp^3 chemisorption), (B) two chains per unit cell (all sp^3 chemisorption), (C) four chains per unit cell (2−2 mode; all sp^3 chemisorption), (D) four chains per unit cell (3−1 mode; all sp^3 chemisorption), (E) four chains per unit cell (2−2 mode; half sp and half sp^3 chemisorption), (F) four chains per unit cell (3−1 mode; $^1/_4$ sp and $^3/_4$ sp^3 chemisorption), (G) four chains per unit cell (1−3 mode; $^3/_4$ sp and $^1/_4$ sp^3 chemisorption).

TABLE 7: $\delta\langle Z_{CH_3}\rangle$ of SAMs Formed by *n*-Alkanethiols on Au(111) at 298 K[a]

initial packing structures: chemisorption modes	$\delta\langle Z_{CH_3}\rangle$
A. 1 chain per unit cell: all sp^3	−0.43 [**1**]
B. 2 chains per unit cell: all sp^3	−0.34 [**2**]
C. 4 chains per unit cell (2−2 mode): all sp^3	−0.43 [**1**]
D. 4 chains per unit cell (3−1 mode): all sp^3	−0.23 [**4**(3−1)]
E. 4 chains per unit cell (2−2 mode): half sp^3 and half sp	0.00 [**4**(2−2)]
F. 4 chains per unit cell (3−1 mode): $^3/_4$ sp^3 and $^1/_4$ sp	−0.23 [**4**(3−1)]
G. 4 chains per unit cell (1−3 mode): $^1/_4$ sp^3 and $^3/_4$ sp	0.22 [**4**(1−3)]

[a] The bold number in the bracket denotes the number of chains per unit cell in packing structure derived from MD simulations. For four chains per unit cell structures, the detailed packing mode is shown in parentheses. $\delta\langle Z_{CH_3}\rangle = \langle Z_{CH_3}\rangle_{C17} - \langle Z_{CH_3}\rangle_{C16}$. Units: $\delta\langle Z_{CH_3}\rangle$, Å.

TABLE 8: $\delta\langle Z_{CH_3}\rangle$ of SAMs Formed by 4′-Alkoxybiphenyl-4-thiols on Au(111) at 298 K[a]

initial packing structures: chemisorption modes	$\delta\langle Z_{CH_3}\rangle$
A. 1 chain per unit cell: all sp	−0.42 [**1**]
B. 2 chains per unit cell: all sp	−0.32 [**2**]
C. 4 chains per unit cell (2−2 mode): all sp	0.00 [**4**(2−2)]
D. 4 chains per unit cell (3−1 mode): all sp	−0.22 [**4**(3−1)]

[a] The bold number in the bracket denotes the number of chains per unit cell in packing structure derived from MD simulations. For four chains per unit cell structures, the detailed packing mode is shown in parentheses. $\delta\langle Z_{CH_3}\rangle = \langle Z_{CH_3}\rangle_{C17} - \langle Z_{CH_3}\rangle_{C16}$. Units: $\delta\langle Z_{CH_3}\rangle$, Å.

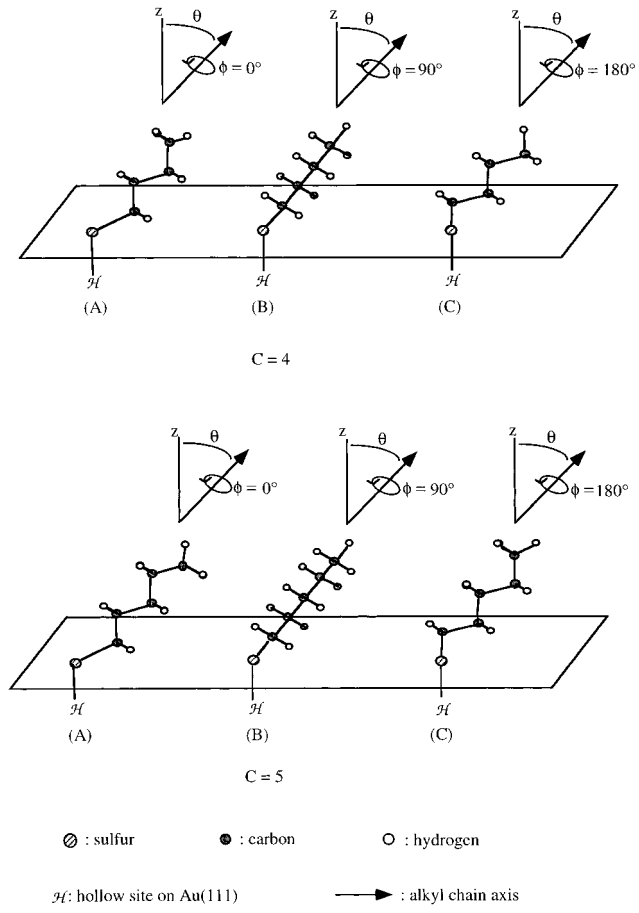

Figure 7. Relationship between the twist of alkyl chains and the *z*-projection of methyl groups with fixed tilt angle for $C = 4$ and 5.

odd−even effect reaches a maximum. When ϕ is 90°, the odd−even effect reaches a minimum, zero. The situation is the same for the negative twists around −90°.

Now, these principles are used to investigate the relationship between $\langle\phi\rangle$ in Table 5 and the odd−even effect, $\delta\langle Z_{CH_3}\rangle$, in Table 7 for different final packing arrangements of *n*-alkanethiols. For one chain per unit cell (simulations A and C in Table 5), all of $\langle\phi\rangle$ are around 38°. For two chains per unit cell (simulation B in Table 5), half of $\langle\phi\rangle$ are around 50° and the other half are around −50°. Although signs of the twists are opposite, the same absolute values indicate the same value for Z_{CH_3}. Here, the absolute values of ϕ for one chain per unit cell and two chains per unit cell are both smaller than 90°. So, the smaller $\langle\phi\rangle$ is, the larger $\delta\langle Z_{CH_3}\rangle$ will be. $\delta\langle Z_{CH_3}\rangle$ of one chain per unit cell is larger than two chains per unit and so is the odd−even effect. For the 2−2 mode of four chains per unit cell packing (simulation E in Table 5), half of $\langle\phi\rangle$ are around 45° and the other half are around 135°. Because half of $\langle\phi\rangle$ are smaller than 90° and the other half are greater than 90°, the odd−even effect of $^1/_2$ *n*-alkanethiols is opposite to that of the other $^1/_2$. Consequently, the odd−even effect is canceled for the packing arrangement of the 2−2 mode of four chains per unit cell packing. For the 3−1 mode of four chains per unit cell packing, because $\langle\phi\rangle$ of $^3/_4$ of the molecules are close to 37° and that of the other $^1/_4$ are close to 130°, its odd−even effect is smaller than that of one chain per unit cell packing. Finally, for the 1−3 mode of four chains per unit cell packing, $\langle\phi\rangle$ of $^3/_4$ of the molecules are close to −140° and that of the other $^1/_4$ are close to −50°, so its odd−even effect is opposite to those of other packing structures and its absolute magnitude of $\delta\langle Z_{CH_3}\rangle$ is also smaller than that of one chain per unit cell. The fact that the $\delta\langle Z_{CH_3}\rangle$ values of 3−1 mode and 1−3 modes listed in Tables 7 and 8 are roughly half of the value of one chain per unit cell packing indicates the simple principles listed above are quite effective.

The calculated Z_{CH_3} (a function of ϕ when θ is fixed) is not only important for differentiating the influence of packing arrangement on odd−even effect observed from reflection IR spectra, but it is also important for linking the MD results with patterns observed in high-resolution STM images.[16,17,38] Figure 8A shows the population of Z_{CH_3} in the 2−2 mode of four chains per unit cell packing of *n*-heptadecanethiol; half of Z_{CH_3} are around 1 Å and their methyl groups tilt close to the surface normal, while the other half are around 0.6 Å and their methyl groups tilt away from the surface normal (Figure 8B). According to the 2×2 supercell in Figure 2C, the inequivalent methyl orientations in the 2−2 mode should result in a zigzag pattern, which is consistent with the zigzag structure shown in Figure 2D of ref 17. Similarly, the surface patterns obtained from the 3−1 and 1−3 modes are consistent with images shown in Figure 2B,C of the same reference.

4.3. Enhanced Odd−Even Effect from *n*-Alkanethiols to 4′-Alkoxybiphenyl-4-thiols. The reflection IR spectra has shown that the odd−even effect of 4′-alkoxybiphenyl-4-thiols on Au(111) was much stronger than that of *n*-alkanethiols. At that time, only one type of packing arrangement (one chain per unit cell packing for both thiols) was taken into consideration, and the twist angles of alkyl chains, ϕ, were in the range between 0° and 90°. The simplified model implied that the larger ϕ was, the weaker the odd−even effect would be. Therefore, one possible explanation of the enhanced odd−even effect was that ϕ of *n*-alkanethiol on Au(111) was larger than that of 4′-alkoxybiphenyl-4-thiol.[22] Why is ϕ of 4′-alkoxybiphenyl-4-thiols on Au(111) smaller than that of *n*-alkanethiols? It was suggested that the rotational barrier of ϕ_{ox} might be at work (the eclipsing effect), which did not occur in the case of *n*-alkanethiols.

In Tables 5 and 6, MD simulation results show that $\delta\langle Z_{CH_3}\rangle$ of one chain per unit cell for *n*-alkanethiols is almost the same

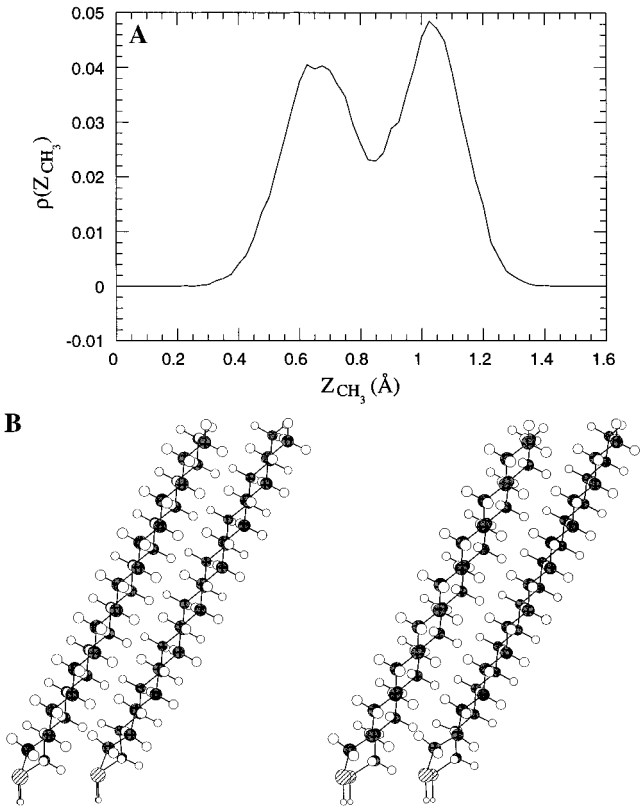

Figure 8. (A) Population profile of the *z*-projection of methyl groups for the final packing structure (MD simulations) of four chains per unit cell (2−2 mode) of *n*-alkanethiols ($C = 16$) at 298 K. (B) Stereoview of a 2−2 mode.

as that of 4′-alkoxybiphenyl-4-thiols, and therefore both thiols have similar odd−even effects. It is noted that $\langle\phi\rangle$ of one chain per unit cell for 4′-alkoxybiphenyl-4-thiols on Au(111) is smaller than that of *n*-alkanethiols, but $\langle\phi\rangle$ of one chain per unit cell for 4′-alkoxybiphenyl-4-thiols on Au(111) is also smaller than that for *n*-alkanethiols. Since the relative magnitude of the odd−even effect is influenced by both $\langle\phi\rangle$ and $\langle\theta\rangle$, the simple principles listed in the last section is not suitable here. It is obvious that if one chain per unit cell is the only packing arrangement, the eclipsing effect does not influence the odd−even effect of the long-chain thiols. According to discussion in the last section, different domains can produce different magnitudes of the odd−even effect, whose order is the following: one chain per unit cell > two chains per unit cell > 3−1 mode of four chains per unit cell > the 2−2 mode of four chains per unit cell (zero odd−even effect) > the 1−3 mode of four chains (opposite odd−even effect). Tables 5 and 6 show that the one chain per unit cell structure is the most favorable packing arrangement for *n*-alkanethiolates and 4′-alkoxybiphenyl-4-thiols on Au(111). The second most favorable domain for *n*-alkanethiols is of the four chains per unit cell packing, including 1−3, 2−2, and 3−1 modes. The two chains per unit cell packing is the least favorable. However, for 4′-alkoxybiphenyl-4-thiols, the second most favorable domain is of the two chains per unit cell packing (due to the eclipsing effect discussed in Section 4.1). Moreover, among its four chains per unit cell packing arrangements, the 1−3 mode (which causes reverse odd−even effect) is not stable. It is conceivable that this difference in preferred domains for *n*-alkanethiols and 4′-alkoxybiphenyl-4-thiols on Au(111) will result in different overall odd−even effects. Since the favored domains of 4′-alkoxybiphenyl-4-thiols on Au(111) possess a larger odd−even effect than that of *n*-alkanethiols, the qualitative prediction based on our MD results is consistent with the enhanced odd−even effect of 4′-alkoxybiphenyl-4-thiols observed in reflection IR spectra.

4.4. Assessment of the Validity and Limit of the Model. In this study we have used a simplified model to treat a complex system, just as has been done repeatedly for solving complicated problems in the real world. It is important to examine closely the basis of the model and the results thus derived. Our model assumes a fixed position for sulfur and a slight preference of sp^3-hybridization over sp-hybridization for the chemisorption structure of sulfur. The fixed model simplification is made because ordered $(\sqrt{3} \times \sqrt{3})R30°$ lattice or superlattice has been observed in STM images. The small preference for sp^3-hybridization is based on the ab initio calculation results and the trend of odd−even effect observed in reflection IR spectra. To some extent, the flexibility lost in our fixed model may have been incorporated into the flexibility of the chemisorption structure of *n*-alkanethiols and the limited movement of the biphenyl group of 4-alkoxybiphenyl-4-thiols. At any rate, the MD results of rigid and flexible 3−1 modes of the four chains per unit cell packing (structures D and F in Table 7 and structure D in Table 8) show virtually the same odd−even effect. Therefore, a more complicated model that includes the local mobility of sulfur on the surface is unlikely to significantly change the odd−even effect of a given packing arrangement. Nevertheless, a more complicated model will likely result in changes of energy difference between different packing arrangements. Since there is some uncertainty in the ab initio results,[39] we do not intend to modify the force field further. We feel that the energy differences between different packing domains may be reduced if a fully relaxed model is adopted. In fact, high-resolution STM images show the coexistence of the $(\sqrt{3} \times \sqrt{3})R30°$ simple lattice and $c(4 \times 2)$ superlattices, with the $(\sqrt{3} \times \sqrt{3})R30°$ simple lattice being the predominant feature.[16] Therefore, the present calculated energy differences between different domains are overestimated.

Although our calculated results are consistent with the enhanced IR odd−even effect and available STM results, there is still one IR result that we have not discussed, that is, the band splittings observed for docosanethiol on Au(111) at 80 K. It has been proposed that the splittings are consistent with a two chains per unit cell packing,[7a] a structure that has not been reported from STM studies. Through our simulations, we found the methyl groups in a two chains per unit cell packing point to different directions, but the Z_{CH_3} are similar (because the twist angles are of the same magnitude and opposite in sign; Table 5). In other words, the density of states experienced by the STM tip could be rather similar for methyl groups in a two chains per unit cell domain. We feel that it is thus more difficult to detect a two chains per unit cell domain than a four chains per unit cell one. Therefore, the existence of the two chains per unit cell packing cannot be excluded. On the other hand, whether the band splittings observed in IR spectra are actually from any of the four chains per unit cell domains remains an interesting question.

The essence of our results is that the *flexibility of the headgroup controls the variety of stable nanodomains on the surface*. Each domain possesses different characteristics which may or may not be discerned by a certain physical measurement. Coupling the experimental evidence with MD simulations, some understanding at the molecular level is achieved. For *n*-alkanethiols on Au(111), the flexibility of the sulfur atom helps to relieve the strain in packing arrangements that have small or

opposite odd−even effects. For 4′-alkoxybiphenyl-4-thiols, the bending flexibility of the sulfur atom is masked by the densely packed biphenyl group. The rigid oxygen headgroup,[40] coupled with the eclipsing effect, makes the available packing arrangements for the alkyl part of 4′-alkoxybiphenyl-4-thiols different from those of *n*-alkanethiols on Au(111) and hence different odd−even effects. We do not feel this general picture will be changed even if a more refined model is used.

5. Summary

We have investigated different packing structures for *n*-alkanethiols and 4′-alkoxybiphenyl-4-thiols on Au(111) and demonstrate their odd−even effect, the molecular orientation, and relative potential energy. The packing arrangements include one, two, and four chains per unit cell (1−3, 2−2, and 3−1 modes). As suggested from the reflection IR spectra, we start the MD simulations with sp^3 chemisorption for *n*-alkanethiols on Au(111) and sp chemisorption for 4′-alkoxybiphenyl-4-thiols. However, with sp^3 chemisorption for *n*-alkanethiols, some four chains per unit cell structures (the 1−3 and 2−2 modes) are unstable and transformed into one chain per unit cell, owing to steric repulsion between the alkyl chains. According to the optimization results, we change some sulfur atoms (with θ_{sul} greater than 120°) to the sp-hybridization structure and obtain stable four chains per unit cell structures (1−3 and 2−2 mode) for *n*-alkanethiols. The tilt angles are similar in all calculated structures, so different twist angles of alkyl chain planes imply different orientations of their methyl groups with respect to surface normal. The patterns of ϕ from MD simulations for four chains per unit cell packing (1−3, 2−2, and 3−1 modes) imply three different contrast variation patterns for the c(4×2) superlattices, which are consistent with those observed by STM for *n*-alkanethiols on Au(111).

The pattern of θ and ϕ from MD simulations also helps us to put forth simple principles to rationalize the odd−even effect for each packing domain. We found the order of odd−even effect is one chain per unit cell > two chains per unit cell > four chains per unit cell. Specifically, the 2−2 mode of the four chains per unit cell packing shows zero odd−even effect, and the 1−3 mode shows opposite odd−even effect to that of the 3−1 mode or any other packing structures. With the information, it is possible to ponder on the larger odd−even effect observed for 4′-alkoxybiphenyl-4-thiols on Au(111) than for *n*-alkanethiols. For *n*-alkanethiols, the flexibility of the sulfur headgroup makes the existence of the 1−3 and 2−2 four chains per unit cell structures possible. In the case of 4′-alkoxybiphenyl-4-thiols on Au(111), the flexibility of sulfur helps the biphenyl part to pack parallel to the surface normal but shows little effect on the packing geometries of the alkyl tails. The effective headgroup that controls the alkyl packing structures of 4′-alkoxybiphenyl-4-thiols is oxygen, which is more rigid than sulfur on gold in terms of bending or torsional angles. This new headgroup disfavors the domains with weak odd−even effect (e.g., the 1−3 mode cannot be located), so the overall odd−even effect of 4′-alkoxybiphenyl-4-thiols on Au(111) is stronger than that of *n*-alkanethiols.

In short, with the aid of simulation results of SAMs on Au(111), one of the controlling factors of SAM structure, the flexibility of the headgroup, has been revealed and analyzed at a molecular level. A relationship between headgroups and alkyl packing structures is established. Finally, one of us have recently looked at the odd−even effect of *n*-alkyldithioic acid on Au(111).[41] The odd−even effect is much stronger than that of *n*-alkanethiols on Au(111), as what one would predict on the basis of the headgroup−structure relationship developed herein.

Acknowledgment. This work was supported by the National Science Council (Grant NSC 84-2113-M-001-033 CT), Republic of China (Taiwan). We are grateful to Prof. Yu-ling Wang for helpful discussion and Dr. J. H. Shih for his assistance in manuscript preparation.

Supporting Information Available: Mulliken charges from AM1 and their performance (Figure S1 and Table S1); typical profiles of potential energy, tilt, and twist with respect to time (Figure S2) (4 pages). Ordering information and accessing is given on any current masthead page.

List of Symbols

C_n = carbon of an alkyl chain; when $n = 1$, the carbon is the one next to the headgroup. The larger n is, the closer to the terminal methyl group it will be.

C_{Ar} = carbon of biphenyl that is close to the oxygen atom

H = hollow site

Z = surface normal of the Au surface

Z_{CH_3} = summation of z-component of $\overrightarrow{CH}$ for the terminal methyl group

Z_{tail} = distance between the terminal methyl group and the Au surface

Greek Letters

ϕ = twist angle of an alkyl chain plane; it is defined as the angle between the alkyl chain plane and the plane formed by Z and the alkyl chain axis, which is made by the headgroup and C_n (n is even). However, to immediately get the precise statistics during MD simulation, ϕ of *n*-alkanethiols is obtained by averaging torsional angles $\angle HSC_{12}C_{13}$ and $\angle HSC_{14}C_{15}$. For 4′-alkoxybiphenyl-4-thiols, ϕ is calculated by averaging torsional angles $\angle HOC_{12}C_{13}$ and $\angle HOC_{14}C_{15}$. (Also see Figure 7.)

ϕ_{ox} = torsional angle of $\angle C_{Ar}C_{Ar}OC_1$

θ = tilt angle of alkyl chain with respect to the surface normal. Here, in order to immediately get the precise statistics during MD simulation, θ of *n*-alkanethiols is obtained by averaging angles $\angle HSC_{12}$ and $\angle HSC_{14}$ and then subtracting the averaged number from 180. For 4′-alkoxybiphenyl-4-thiols, θ is calculated by averaging angles $\angle HOC_{12}$ and $\angle HOC_{14}$. (Also see Figure 7.)

$\theta°$ = equilibrium bond angle

θ_{ox} = bond angle of $\angle C_{Ar}OC_1$

θ_{sul} = bond angle of $\angle HSC_1$

References and Notes

(1) Bain, C. D.; Whitesides, G. M. *Angew. Chem., Int. Ed. Engl.* **1989**, *28*, 506.

(2) Whitesides, G. M.; Laibinis, P. E. *Langmuir* **1990**, *6*, 87.

(3) Laibinis, P. E.; Nuzzo, R. G.; Whitesides, G. M. *J. Phys. Chem.* **1992**, *96*, 5097.

(4) Ulman, A. *An Introduction to Thin Organic Films: From Langmuir−Blodgett to Self-Assembly*; Academic Press: Boston, MA, 1991.

(5) Prasad, P. N.; Williams, D. *Introduction to Nonlinear Optical Effects in Molecules and Polymers;* Wiley-Interscience: New York, 1991.

(6) (a) Jackman, R. J.; Wilbur, J. L.; Whitesides, G. M. *Science* **1995**, *269*, 664. (b) Wolf, M. O.; Fox, M. A. *Langmuir* **1996**, *12*, 955.

(7) (a) Nuzzo, R. G.; Korenic, E. M.; Dubois, L. H. *J. Chem. Phys.* **1990**, *93*, 767. (b) Nuzzo, R. G.; Dubois, L. H.; Allara, D. L. *J. Am. Chem. Soc.* **1990**, *112*, 558.

(8) Bryant, M. A.; Pemberton, J. E. *J. Am. Chem. Soc.* **1991**, *113*, 8284.

(9) (a) Rovida, G.; Pratesi, F. *Surf. Sci.* **1981**, *104*, 609. (b) Strong, L.; Whitesides, G. M. *Langmuir* **1988**, *4*, 546.

(10) (a) Fenter, P.; Eisenberger, P.; Liang, K. S. *Phys. Rev. Lett.* **1993**, *70*, 2447. (b) Camillone, N., III; Chidsey, C. E. D.; Eisenberger, P.; Fenter, P.; Li, J.; Liang, K. S.; Liu, G.-Y.; Scoles, G. *J. Chem. Phys.* **1993**, *99*, 744.

(11) Camillone, N., III; Chidsey, C. E. D.; Liu, G.-y.; Scoles, G. *J. Chem. Phys.* **1993**, *98*, 3503.

(12) Alves, C. A.; Smith, E. L.; Porter, M. D. *J. Am. Chem. Soc.* **1992**, *114*, 1222.

(13) Widrig, C. A.; Alves, C. A.; Porter, M. D. *J. Am. Chem. Soc.* **1991**, *113*, 2805.

(14) Poirier, G. E.; Tarlov, M. J. *Langmuir* **1994**, *10*, 2853.

(15) Poirier, G. E.; Tarlov, M. J.; Rushmeier, H. E. *Langmuir* **1994**, *10*, 3383.

(16) Delamarche, E.; Michel, B.; Gerber, C.; Anselmetti, D.; Güntherodt, H.-J.; Wolf, H.; Ringsdorf, H. *Langmuir* **1994**, *10*, 2869.

(17) Anselmetti, D.; Baratoff, A.; Güntherodt, H. J.; Delamarche, E.; Michel, B.; Gerber, C.; Kang, H.; Wolf, H. *Europhys. Lett.* **1994**, *27*, 365.

(18) Mar, W.; Klein, M. L. *Langmuir* **1994**, *10*, 188.

(19) Sellers, H.; Ulman, A.; Shnidman, Y.; Eilers, J. E. *J. Am. Chem. Soc.* **1993**, *115*, 9389.

(20) Pertsin, A. J.; Grunze, M. *Langmuir* **1994**, *10*, 3668.

(21) Hautman, J.; Klein, M. L. *J. Chem. Phys.* **1990**, *93*, 7483.

(22) Chang, S.-C.; Chao, I.; Tao, Y.-T. *J. Am. Chem. Soc.* **1994**, *116*, 6792.

(23) Dhirani, A.-A.; Zehner, R. W.; Hsung, R. P.; Guyot-Sionnest, P.; Sita, L. R. *J. Am. Chem. Soc.* **1996**, *118*, 3319.

(24) Spellmeryer, D. C.; Grootenhuis, P. D. J.; Miller, M. D.; Kuyper, L. F.; Kollman, P. A. *J. Phys. Chem.* **1990**, *94*, 4483.

(25) Lii, J.-H.; Allinger, N. L. *J. Am. Chem. Soc.* **1989**, *111*, 8576.

(26) Walczak, M. M.; Chung, C.; Stole, S. M.; Widrig, C. A.; Porter, M. D. *J. Am. Chem. Soc.* **1991**, *113*, 2370.

(27) We have studied short-chain *n*-alkanethiols and 4′-alkoxybiphenyl-4-thiols ($C = 4, 5$) with a ($\sqrt{3} \times \sqrt{3}$) lattice, which is the fundamental binding site of SAMs on Au(111), and did not find any conclusive results to explain the diminishing odd−even effect from the short-chain thiols to long-chain thiols. A recent STM observation showed that it took 50 h for butanethiols on Au(111) to grow into a saturated complex domain of packing patterns. And, the basic repeat unit of the saturated packing structure is the $p \times \sqrt{3}$ superlattice, where $8 \leq p \leq 10$ or p can be 7. Therefore, either before or after the saturated crystallization, the packing space of butanethiols on Au(111) is larger than the fundamental ($\sqrt{3} \times \sqrt{3}$) space of SAMs on Au(111). Owing to the uncertainty of the packing space, a precise energy function to describe the mobility of SAMs on Au(111) is important. However, up to now, there is still no good energy function to describe it. References for STM observation of liquidlike SAMs on Au(111) are the following: Poirier, G. E.; Tarlov, M. J. *J. Phys. Chem.* **1995**, *99*, 10966. Kang, J.; Rowntree, P. A. *Langmuir* **1996**, *12*, 2813.

(28) Mayo, A. L.; Olafson, B. D.; Goddard, W. A., III. *J. Phys. Chem.* **1990**, *94*, 8897.

(29) Dewar, M. J. S.; Zoebisch, E. G.; Healy, E. F. *J. Am. Chem. Soc.* **1985**, *107*, 3902.

(30) Cerius^2, version 2.0, BIOSYM/Molecular Simulations Inc., 1995.

(31) Sabatani, E.; Cohen-Boulakia, J.; Bruening, M.; Rubinstein, I. *Langmuir* **1993**, *9*, 2974.

(32) Nosé, S. J. *J. Chem. Phys.* **1984**, *91*, 511.

(33) Siepmann, J. I.; McDonald, I. R. *Langmuir* **1993**, *9*, 2351.

(34) Our calculations showed that the most favored packing domain for both types of thiols is one chain per unit cell. This is different from the results obtained by Mar and Klein for *n*-alkanethiol ($C = 15$), in which two chains per unit cell was shown as the lowest-energy packing structure. It is possibly because our model includes electrostatic interaction for the alkyl part; when electrostatic interaction was turned off, we also found two chains per unit cell as the lowest-energy packing structure.

(35) We also find the packing structure of four chains per unit cell (1−3 mode) for *n*-alkanethiols with only sp^3 chemisorption and for 4′-alkoxybiphenyl-4-thiols. Their minimized ΔE values are two (to three) times higher than that for other packing structures. Furthermore, these packing structures are all unstable at 298 K and changed into either one chain per unit cell or two chains per unit cell during MD simulations.

(36) Since the packing parameters (θ, ϕ) of the alkyl part of the aromatic-derivatized thiols are similar to that of *n*-alkanethiols, the energy difference estimation was based on the potential energy difference of structures A and B of *n*-alkanethiols (Table 2).

(37) Typical profiles of MD results with respect to time can be found in the Supporting Information section.

(38) We suggest that the contrast variations observed in the STM images of the superlattices, c(4×2), were due to the different orientation of the methyl group of SAMs and could be related to $\langle Z_{CH_3} \rangle$.

(39) For example, the model used in the ab initio study involves a cluster in which the Au atoms are not allowed to relax upon sulfur binding.

(40) We are convinced that the bending flexibility of sulfur on gold is larger than that of oxygen in an organic moiety in view of the participation of multiple gold atoms in a Au(surface)−S bond (see ref 19). The gold atoms can fulfill different bonding demands of sulfur in different Au−S−C bending angles more easily than the neighboring groups of oxygen in alkoxybiphenylthiols can. Therefore, the low energy difference and barrier calculated by Sellers (ref 19) for sulfur angle variation is reasonable.

(41) Tao, Y.-T.; Pandiaraju, S.; Lin, W. L. Paper in preparation.